

NATIONAL AERONAUTICS AND SPACE ADMINISTRATION

Technical Memorandum 33-673

*Uncertainties in Predicting Solar
Panel Power Output*

Bruce Anspaugh

(NASA-CR-138455) UNCERTAINTIES IN
PREDICTING SOLAR PANEL POWER OUTPUT (Jet
Propulsion Lab.) #7 p HC \$5.50 CSCL 10A

52

N74-22710

Unclas

G3/03 39745

JET PROPULSION LABORATORY
CALIFORNIA INSTITUTE OF TECHNOLOGY
PASADENA, CALIFORNIA

April 15, 1974

NATIONAL AERONAUTICS AND SPACE ADMINISTRATION

Technical Memorandum 33-673

*Uncertainties in Predicting Solar
Panel Power Output*

Bruce Anspaugh

JET PROPULSION LABORATORY
CALIFORNIA INSTITUTE OF TECHNOLOGY
PASADENA, CALIFORNIA

April 15, 1974

°
/

Prepared Under Contract No. NAS 7-100
National Aeronautics and Space Administration

PREFACE

The work described in this report was performed by the Guidance and Control Division of the Jet Propulsion Laboratory.

PRECEDING PAGE BLANK NOT FILMED

CONTENTS

I.	Introduction	1
II.	Panel Assembly Power Losses	5
III.	General Error Discussion	8
IV.	Cell Measurement Uncertainty at the Cell Manufacturer's Facility	12
V.	Uncertainties in the Solar Panel Calibration at Table Mountain	20
VI.	Predicting Panel Output in Space	24
	A. Correction for Solar Intensity and Panel Temperature	24
	B. Calculation of a Mission Profile	33
VII.	Recommendations.	38
	References	39

LIST OF TABLES

I.	Sources of solar panel uncertainty	32
----	----------------------------------------------	----

LIST OF FIGURES

1.	Current at 0.485 volts, distribution for 2-ohm-cm cells	41
2.	Short circuit current distribution of 10-ohm-cm solar cells before and after glassing with 6-mil microsheet	41
3.	Short circuit current distribution of 2-ohm-cm solar cells before and after glassing with 6-mil 7940 fused silica	42
4.	Current reduction after coverslide mounting (2 x 2 cm cells)	42

CONTENTS (contd)

5.	Current reduction after coverslide mounting (2 x 4 cm cells)	43
6.	95% current confidence band on a 2-ohm-cm solar cell	43
7.	$\alpha = (\partial I_{sc} / \partial T)_H$ based on differentiating Patterson's expression	44
8.	$(\partial V_{oc} / \partial T)_H$ based on differentiating Patterson's expression	44
9.	$(\partial V_{oc} / \partial H)_T$ based on differentiating Patterson's expression	45
10.	Portion of 2-ohm-cm solar cell I-V curve near P_{max} for AMO, 28°C	45

ABSTRACT

This report examines the problem of calculating solar panel power output at launch and during a space mission. It also examines the major sources of uncertainty and error in predicting the post launch electrical performance of the panel. A general discussion of error analysis is given. Examples of uncertainty calculations are included. A general method of calculating the effect on the panel of various degrading environments is presented, with references supplied for specific methods. A technique for sizing a solar panel for a required mission power profile is developed.

SECTION I

INTRODUCTION

This memorandum presents calculational procedures for predicting the power output of a solar panel throughout its life. It shows how to determine the power output of a freshly manufactured solar panel, of a panel immediately after launch, and of a panel after exposure to the rather poorly known space environments, which may include radiation, ultraviolet exposure, temperature excursions and changes in incident solar intensity. Uncertainties in making the predictions are detailed and a method of calculating the overall uncertainty in panel performance is presented. The prediction uncertainty is the main subject treated in this paper. The problem is separated into two broad categories: (1) prediction of panel performance immediately after launch and (2) prediction thereafter.

Post launch environments affecting the panel output which are amenable to treatment by the techniques in this paper include solar intensity, panel temperature, electron and proton irradiation arising either from the Van Allen belts or solar flares, ultraviolet degradation of the coverslide optical system, micrometeoroid irradiation, and the effect of thermal cycling.

A summary of the factors treated in this paper which contribute to the uncertainty in predicting array space performance include:

- 1) Errors in cell measurement which contribute to cell matching loss
- 2) Effects of coverslide filtering
- 3) Manufacturing losses due to soldering, wiring, etc.
- 4) Calibration of the balloon flight standard solar cells
- 5) Prelaunch Table Mountain (Earth sunlight) measurements of space solar arrays
- 6) Uncertainties in the JPL computer program for predicting panel performance in space

- 7) The following damaging environments to which the array will be exposed in space. (The effect of these environments is a function of the spacecraft mission parameters and the solar array design):
- a) Ultraviolet radiation
 - b) Micrometeoroid impact
 - c) Van Allen belt radiation
 - d) Solar flare protons
 - e) Thermal cycling

All the uncertainties due to prelaunch measurements and calibration are combined to calculate an uncertainty in the predicted panel output just after launch. The methods of predicting solar panel output as panel temperature and incident solar intensity change used in the JPL computer program M132000 are described and criticized. The errors in using the methods in the program are analyzed, tabulated and combined. An example of an error calculation for a panel like the Mariner '71 Mars orbiter solar panel is presented. Recommendations are given which are designed to decrease the panel assembly losses and reduce the panel prediction uncertainties.

Using the JPL M132000 computer program to predict the panel output, an uncertainty in the prediction of I_{sc} , V_{oc} , and P_{max} may be computed as follows:

$$\left(\frac{dI_p}{I_p}\right)^2 = \left(\frac{dH}{H}\right)^2 + \left(\frac{\alpha_o dT_t}{I_t}\right)^2 + \left(\frac{nodT_p}{I_p}\right)^2 + \left(\frac{dI}{I}\right)_{TM}^2 + S_I^2 + e_I^2$$

$$\left(\frac{dV_{oc}}{V_{oc}}\right)^2 = \left(\frac{1}{V_{oc}} \frac{\partial V_{oc}}{\partial T} dT_t\right)^2 + \left(\frac{1}{V_{ocp}} \frac{\partial V_{ocp}}{\partial T} dT_p\right)^2$$

$$+ \left(\frac{1}{V_{ocp}} \frac{\partial V_{ocp}}{\partial H} dH\right)^2 + \left(\frac{dV_{ocp}}{V_{ocp}}\right)^2 + S_V^2 + e_V^2$$

$$\left(\frac{dP_m}{P_m}\right)^2 = \left(\frac{dV_{oc}}{V_{oc}} \frac{V_{oc}}{V_{mp}}\right)^2 + \left(\frac{dI_{sc}}{I_{sc}} \frac{I_{sc}}{I_{mp}}\right)^2$$

The terms appearing in the above equations are defined below:

I_t = cell current during parametric data acquisition at (H, T_t),
mA

I_p = panel current, mA

H = solar intensity at which solar cell output is predicted,
 mW/cm^2

dH = solar intensity uncertainty including simulator intensity
uncertainty when the parametric solar cell data used in
M132000 was acquired and the uncertainty of the solar
intensity incident on the spacecraft.

α_o = temperature coefficient of short circuit current at the
nearest tabulated (H, T) point in M132000 to the desired
intensity and panel temperature, $\text{mA}/^\circ\text{C}$.

α = same as α_o , but at the desired intensity and panel
temperature

dT_t = cell temperature uncertainty during parametric data
acquisition $^\circ\text{C}$

dT_p = panel temperature uncertainty, $^\circ\text{C}$

n = number of cells in parallel on the panel

$\left(\frac{dI}{I}\right)_{TM}$ = uncertainty in measuring solar panel current at Table
Mountain

S_I = statistical 95 percent confidence limit of the parametric
current data, mA

e_I = current prediction error of M132000, mA

V_{ocp} = panel open circuit voltage, mV

V_{oc} = single cell open circuit voltage, mV

m = number of cells in series on the panel

$\left(\frac{dV_{ocp}}{V_{ocp}}\right)_{TM}$ = uncertainty in measuring the solar panel voltage at
Table Mountain

S_v = statistical 95 percent confidence limit of the parametric
voltage data, mV

e_v = voltage prediction error of M132000, mV

P_m = panel maximum power, mW

V_{mp} = voltage at maximum power, mV

I_{mp} = current at maximum power, mA.

In the example calculations the uncertainties in predicting I_{sc} , V_{oc} , and P_{max} at 100 mW/cm^2 and 0°C were calculated for a Mariner '71 panel. At the 95 percent confidence level they are 2.49 percent for I_{sc} , 2.26 percent for V_{oc} and 3.82 percent in P_{max} .

SECTION II

PANEL ASSEMBLY POWER LOSSES

Solar cells for a particular project are purchased to a specification which imposes some restriction on the power output of each cell. The restriction is usually applied to solar cell current at a constant voltage because this is a relatively easy measurement to make on the assembly line and can be a fairly good approximation to the cell maximum power. A distribution function for the cell power can be obtained from a proper sampling of the total population of solar cells manufactured for that project. Means and standard deviations can be estimated. Such a distribution for Lots 1B through 5 of the Mariner 9 (interchangeably referred to in this paper as Mariner '71) solar cells is shown in Figure 1. These cells were 1 to 3 ohm-cm and measured 2 x 2 x 0.046 cm. The distribution shown is for 1000 cells sampled at the manufacturer's plant and is plotted for cell current at a voltage of 0.485 volts.

At this point several things are done to the solar cells in the process of assembling them into a panel which change the power distribution function. Data regarding the changes to the distribution function as the cells are processed is difficult to find. The cells are sorted by the manufacturer into output current groupings of 2 mA. A sampling of the output lot is taken at the manufacturer's facility for the purpose of establishing the overall current distribution, averages, standard deviations, and to determine if the cells will pass their required environmental tests. If a lot of cells is satisfactory, the assembly of submodules is begun. A submodule consists of a number, p , of cells (4 or 5 on Mariner '71) which are connected in parallel. The cells comprising a submodule are selected so that the submodule current output (at reference voltage) will be p times the average output current. If each submodule has nearly the same current output near operating voltage, no one single submodule will act as a load when the submodules are later connected into a series string. Coverglasses are now applied. In order to insure that the submodules will have matching current outputs even after the application of the coverglasses, the current output of each submodule is remeasured. The practice at this laboratory has been to measure the submodules in tungsten light after glassing. The submodules are then

connected by a series/parallel arrangement into sections and the sections connected together to match the input impedance requirements of the spacecraft power conditioning system.

It is clear that several or all of the above steps change the current output of the solar cells. The maximum power output of a typical solar panel built for JPL missions is known to be some 6 percent lower than that computed by multiplying the number of cells on the panel by the average power output of a single cell. Some data on the losses due to glassing will be presented in the following paragraphs, but no data could be found on the effect of soldering interconnects onto the cells, the effect of the cell loading due to the mismatch in submodule current output or in the errors made by matching submodules after glassing on the basis of performance in tungsten light.

A large portion of the manufacturing loss occurs when the coverglasses are attached. Cell vendors were cooperative in furnishing data regarding these losses. One vendor furnished complete I-V curves for 128 solar cells (N/P, 7-14 ohm-cm, 2 x 2 x 0.025 cm (10 mils thick)) both before and after installation of 0.15 mm (6 mil) microsheet coverglasses; the other vendor furnished data on 100 solar cells (N/P, 1-3 ohm-cm, 2 x 4 x 0.03 cm (12 mils thick)) before and after glassing with 0.15 mm (6 mil) 7940 fused silica coverglasses. All cells were coated with a SiO coating. The short circuit current distribution for both types of cells both before and after glassing is shown in Figures 2 and 3. Superimposed on the histograms of current distribution are Gaussian curves having the same means and standard deviations. Chi-square tests at the 95 percent confidence level of the 2 x 2 cm cell data showed that the current distributions of the bare cells fit a Gaussian distribution, but did not after glassing. The 2 x 4 cm cells fit Gaussians both before and after glassing. The average I_{sc} loss for the 2 x 2 cells is 3.658 mA or 2.66 percent when glassed with 6 mil microsheet. The average I_{sc} loss for the 2 x 4 cells is 5.577 mA or 1.97 percent. The percentage loss for cells covered with 7940 fused silica is less, as is to be expected, because of the lesser light transmission of the microsheet. Figure 4 is a scatter plot of the 2 x 2 cm cell short circuit current loss as a function of initial short circuit current. The losses have a wide scatter and are unpredictable. The standard deviation in cell loss is

1.28 mA. Figure 5 is a similar plot for the 2 x 4 cm cells. Figure 5 is plotted with both scales twice that of the scales used in Figure 4 for the 2 x 2 cells. Here the scatter is less. The standard deviation of the cell loss is 1.43 mA. Both vendors offered the opinion that the scatter in the loss data is primarily due to variations in the SiO coating which affect the absorption of light in the coating as well as its index of refraction. There are too many uncontrolled variables in these data to draw conclusions as to whether cells glassed with 7940 have less current loss scatter than cells glassed with microsheet. The data on the 2 x 4 cm cells was obtained under unusually intense scrutiny of the people applying the coverglasses, while the same may not have been true for the 2 x 2 cm cells. The cells are of different resistivities, different sizes, may have had different cutoff frequencies for the ultraviolet filters, different coverglass adhesives, or at least different batches of the same adhesive, etc. It is clear however that there is a large scatter in the current loss data and cells which were matched on the basis of preglassing current output for the purpose of assembly into modules will have a significant mismatch after glassing. This loss and the resulting mismatch will account for at least 1.97 percent of the manufacturing losses when 6 mil coverglasses are used and more when thicker coverslides are used. It is possible that this transmission loss and mismatch thereafter may account for the entire 6 percent loss seen in recent Mariner panels when 20 mil coverslides were used.

It is recommended that the cells be glassed prior to measuring the output current for matching purposes. One of the vendors also suggested that the use of a TiO_x antireflection coating would cut down the size and scatter of the current loss since this material has an index of refraction which more nearly matches Si than does SiO. It is therefore further recommended that an investigation be initiated for the purpose of determining why there is so much scatter in the current loss due to glassing, and to try to find ways, including the use of TiO_x antireflection coatings, to reduce the scatter.

SECTION III

GENERAL ERROR DISCUSSION

A large portion of the remainder of this paper will involve discussions of measurement errors and their propagation. This section will discuss philosophy and methodology to be used in that regard.

An excellent discussion of errors and uncertainties is given by Kline and McClintock in Reference 1. A brief summary of a few of their points follows.

Uncertainty is defined to be the possible value the error might have. Note the distinction between error and uncertainty. The difference between the true value in an observed variable and the observed value is the error in that observation. The uncertainty, however, is what an observer thinks the error might be.

An error frequency distribution function can be constructed to describe the errors if a large number of measurements of a variable can be made. Such error frequency functions are often non-Gaussian, but they almost always show that small errors are more likely than big ones, positive and negative errors are about equally probable, and there is no finite upper limit to the possible size of an error. In spite of this, design documents often specify maximum errors or uncertainties. Such numbers should be regarded as highly suspect. It is seldom possible to measure the uncertainty distributions of all the components contributing to the uncertainty of a variable, and another method of describing the uncertainty is required. One method of quoting the best estimate of the value of a variable and the associated measurement error is to give the mean m (arithmetic mean of observed values) and an uncertainty interval w based on specified odds, b . Thus a variable might be quoted as

$$m \pm w (b \text{ to } 1)$$

which means that the observer is willing to wager odds of b to 1 that the true value lies between $m - w$ and $m + w$. The larger the w , the longer the odds one can safely wager. Expressed another way, this interval of width $2w$ centered on m has a probability of $b/(b + 1)$ of containing the true value of the variable.

Let an observation R be the function of n independent variables

$$R = R(v_1, v_2, \dots, v_n) \quad (1)$$

If the variables v_i are normally distributed, with uncertainties w_i associated with each v_i , and all w_i have the same odds, then the uncertainty interval w_R for the result having the same odds is given by

$$w_R = \left[\left(\frac{\partial R}{\partial v_1} w_1 \right)^2 + \left(\frac{\partial R}{\partial v_2} w_2 \right)^2 + \dots + \left(\frac{\partial R}{\partial v_n} w_n \right)^2 \right]^{1/2} \quad (2)$$

This equation gives results that are very nearly correct even when used with uncertainty distribution functions that are grossly non-normal (e. g., 15 percent error for a triangular distribution). This is quite a remarkable result in that it holds for distributions which have uncertainty distributions with finite limits such as the triangular distribution. In view of the fact that uncertainty intervals for the variables are not usually known to better than 50 percent, the use of equation (2) is not unreasonable.

To make use of the uncertainty interval based on odds as discussed by Kline and McClintock, we make use of the statistical confidence limit. Suppose we have a sample population distributed normally, whose true mean μ and true variance σ^2 are somehow known. If we draw a sample of size n at random from this population and calculate a mean \bar{x} from this sample, we can calculate a confidence interval which has a probability $(1 - \alpha)$ of containing the true sample mean. This interval is commonly called a $100(1 - \alpha)$ percent confidence interval. The bounds of the interval are given by

$$\bar{x} \pm Z \frac{\sigma}{\sqrt{n}} \quad (3)$$

In gambling language, the odds are b to 1 that this interval contains the true mean μ . b and α are related by $b = (1 - \alpha)/\alpha$. The α used here is a common notation symbol in statistics texts to describe confidence limits and is not to be confused with the α commonly used by photovoltaics engineers in describing

the temperature coefficient of solar cell short circuit current. $Z_{\alpha/2}$ is the value in the standard normal distribution such that the probability of a random deviation greater than $\pm Z_{\alpha/2}$ is α , i. e.

$$\int_{-\infty}^{-Z_{\alpha/2}} f(Z) dZ + \int_{Z_{\alpha/2}}^{\infty} f(Z) dZ = \frac{\alpha}{2} + \frac{\alpha}{2}$$

where

$$f(Z) = \frac{1}{\sqrt{2\pi}} e^{-\frac{Z^2}{2}} \quad \text{and} \quad Z = \frac{x - \mu}{\sigma}$$

If we are using 95 percent confidence limits, $\alpha = 0.05$ and $Z_{\alpha/2} = 1.96$, and our interval is $\bar{X} \pm 1.96\sigma/\sqrt{n}$. This interval has odds of 19 to 1 for containing the real population mean μ .

Suppose our samples are drawn from a population just like the one in the example above except that the variance is not known. In this event, which is the usual situation encountered in the real world, we typically estimate the variance with a value s^2 found from a random sample of size n as follows:

$$s^2 = \frac{1}{n-1} \sum_{i=1}^n (x_i - \bar{x})^2$$

or equivalently

$$s^2 = \frac{1}{n(n-1)} \left[n \sum_{i=1}^n x_i^2 - \left(\sum_{i=1}^n x_i \right)^2 \right] \quad (4)$$

It is most important to note that the factor of 1.96 used in the previous example will no longer insure 95 percent confidence limits. A bigger factor is needed

because s^2 is only an approximation for σ^2 . In this case the $100(1-\alpha)$ percent confidence limits are

$$X \pm \frac{\left(t_{\frac{\alpha}{2}, n-1}\right) s}{\sqrt{n}} \quad (5)$$

Here, $t_{\alpha/2, n-1}$ is the integral of the Student t distribution (from t to ∞) for $n-1$ degrees of freedom. This distribution is tabulated in most statistics books. For $n = \infty$, $t_{.025, \infty} = 1.96$, coinciding with our previous result for known variance, and suggesting that if we could draw an infinite sample size we could compute an accurate s . If we drew a sample of size 5, however, we would have $t_{.025, 4} = 2.776$ as the multiplier of s/\sqrt{n} .

One often hears the terms 1σ , 2σ , or 3σ levels or limits used in a rather cavalier fashion in conjunction with engineering data. The implication usually is taken that formula (3) can be used to set confidence limits. This is rarely the case however, and equation (5) must be applied. Further discussion of these points along with examples of their application can be found in References (2) and (3).

SECTION IV

CELL MEASUREMENT UNCERTAINTY AT THE CELL MANUFACTURER'S FACILITY

We consider that the solar cell manufacturer has set up his simulator to measure the current output of a batch of solar cells from his assembly line. He is following the requirements of the specifications such as those detailed in Reference 4. This is done by using a standard solar cell called a secondary working standard which is placed in a temperature controlled holding fixture with integral spring loaded contacts. The standard cell is brought to the required temperature of 28°C and the solar simulator intensity adjusted until the short circuit current output of the standard cell attains its calibration value for one solar constant. But, due to uncertainties in the calibration and measurement process, he has probably not actually achieved the desired simulator intensity, H_0 , or the desired temperature, T_0 . Instead the simulator is set at an intensity of $H_1 = H_0 + dH$ and the standard cell is set at a temperature of $T_1 = T_0 + dT$. If we knew absolutely what H_1 and T_1 were, we could correct the simulator intensity by changing the short circuit current of the standard cell an amount

$$dI = \frac{\partial I}{\partial H} dH + \frac{\partial I}{\partial T} dT$$

or

$$\frac{dI}{I} = \frac{dH}{H} + \alpha_0 \frac{dT}{I} \quad (6)$$

if dH and dT are small. Equation (6) assumes that $I = \text{const.} \times H$, so that $(1/I) (\partial I / \partial H) = 1/H$. α_0 is the temperature coefficient of short circuit current at intensity H_0 and temperature T_0 . (Uncertainties in the value of α_0 contribute negligibly to dI/I and are neglected.) An alternative interpretation to equation (6) is that the uncertainty in intensity may be written as

$$\frac{dH}{H} = \frac{dI}{I} - \frac{\alpha_0 dT}{I} \quad (7)$$

with dI representing the possible error the standard cell current may have because of uncertainties in the chain of measurements involved in its calibration.

Uncertainties in the current calibration begin to arise with the calibration of the balloon flight standard cells (BFS) which are flown by JPL on a balloon at altitudes of 24.38 m (80,000 ft) or higher. These cells are loaded with integral precision 1 ohm resistors (0.1 percent) and the voltage drop telemetered to a receiving station. One resistor is used on a 1 x 2 cm cell and 2 resistors in parallel are used on the 2 x 2 cm cells. The cells are recovered after the balloon flight and used in the laboratory as a transfer standard. It does not matter what the accepted value of the solar constant at air mass zero (AMO) is, nor does it matter what the actual value of the load resistor is as long as it is stable, has a low temperature coefficient, and loads the cell near short circuit condition. If the BFS cell is put into a solar simulator beam whose spectrum is a reasonable approximation to that of the sun, and the simulator adjusted to give the same voltage drop across the BFS load resistor as it had at 24.38 (80,000 ft.) with the cell at the same temperature, we have used the BFS to transfer the AMO intensity into the laboratory. In performing this transfer, the sources of error are errors in the voltage read-out and temperature control system during the ballon flight, and voltmeter and cell temperature measurement errors at time of use in the laboratory.

The solar cell vendor does not use a BFS cell to set the intensity of his simulator, however. The JPL specification of reference 4 allows the vendor to use a cell called a secondary working standard (SWS) to set the simulator intensity. This SWS cell is calibrated against a BFS cell, but in doing so, a certain loss of accuracy occurs. A freshly calibrated BFS cell is considered to be accurate to $\pm 1/2$ percent (95 percent confidence limit), but degrades as it is used extensively in the laboratory to an estimated ± 1 percent. The SWS calibration is taken to be ± 2 percent (95 percent confidence limit). The temperatures of the BFS and SWS cells are commonly held to $\pm 1^\circ\text{C}$ which can introduce approximately 0.1 percent uncertainty in the intensity when a 2 ohm cm standard cell is used. The BFS and SWS cells are read with a digital voltmeter assumed to be accurate to ± 0.1 mV out of approximately 60 mV. An additional uncertainty of 0.2 mV is assigned due to difficulties in reading

the cell current because the simulator intensity has short term fluctuations caused by the dancing of the arc in the xenon arc lamp. We therefore assign an uncertainty of 0.5 percent to the voltmeter readings. Using a SWS cell to set up the intensity of the simulator, and if the SWS cell reads exactly the calibrated value, a total uncertainty in the simulator intensity may be calculated using equation (2) as follows:

$$\frac{dH}{H} = \left[(0.02)^2 + (0.001)^2 + (0.005)^2 \right]^{1/2} \times 100 = 2.064\% \quad (8)$$

In addition to the BFS and SWS calibration uncertainties, the solar cell manufacturer is allowed to set his simulator intensity to within ± 2 percent of AMO (Reference 4). It is not known how often the manufacturer recalibrated the light source intensity during a day's series of measurements, but the manufacturer's specification for the X-25 solar simulator quotes a ± 1 percent intensity variation to be possible over a time period of 60 minutes. Assuming these additional uncertainties to be 95 percent confidence limits, we can compute via equation (2) the total uncertainty in the simulator intensity to be

$$\frac{dH}{H} = \left[(0.02064)^2 + (0.02)^2 + (0.01)^2 \right]^{1/2} \times 100 = 3.04\% \quad (9)$$

The solar cell vendor now proceeds to read the current output of his batch of solar cells. The uncertainty in the cell current output is given by equation (6), with the additional uncertainties of the current measuring device factored in. The current is read by using a digital voltmeter to read the voltage drop across a precision resistor, R_c . The current uncertainty introduced by the voltmeter and resistor is

$$\frac{dI_m}{I_m} = \frac{dV}{V} - \frac{dR_c}{R_c} \quad (10)$$

where dI_m represents the uncertainty inherent in the current meter alone. We assume the manufacturer uses a 0.1 percent resistor and a digital voltmeter

with a calibration uncertainty of ± 1 digit in the least significant place (1 part out of 1200 when measuring currents near 120 mA at the 485 mV point). Again the xenon arc light will flicker and give an uncertainty of approximately 2 digits in the least significant place. The total uncertainty of the current reading device is computed by the scheme of equation (2) to be

$$\frac{dI_m}{I_m} = \left[(0.001)^2 + \left(\frac{3}{1200} \right)^2 \right]^{1/2} \times 100 = 0.27\% \quad (11)$$

Using equations (2), (6) and (11), the uncertainty in the solar cell current at $V = 485$ mV is computed as follows:

$$\frac{dI}{I} = \left[(0.0304)^2 + \left(\frac{0.11 \times 1}{120} \right)^2 + (0.0027)^2 \right]^{1/2} \times 100 = 3.05\% \quad (12)$$

assuming that the manufacturer is able to maintain the cell temperatures within 1°C . The nature of this uncertainty is to define a 95 percent confidence band on the solar cell I-V curve by adding $\pm \Delta I$ to each point on the curve such that $\Delta I = 0.0305 \times I_{sc}$. Such a band is shown on a typical Mariner '71 cell in Figure 6.

The spectral content of the test light source can also affect the output of a solar cell. However, according to tests reported by R. Mueller (Ref. 5), quite wide variations in simulator spectral content did not induce directly dependent changes in solar cell output when considering cells of the same type and resistivity. The cell manufacturer was required by contract to use reasonable care in furnishing a simulator spectrum matching the Sun's output so we assume minor spectral fluctuations had no effect.

The α values used in the above equations are calculated from the empirical formulae developed by Patterson et al (Reference 6). For 2 ohm-cm cells, $2 \times 2 \times 0.046$ cm, I_{sc} is expressed as

$$I_{sc} = C(T) H$$

where

$$C(T) = c_0 + c_1 T + c_2 T^2 + c_3 T^3 + c_4 T^4 + c_5 T^5$$

and

$$\begin{aligned} c_0 &= 0.914727 & c_3 &= 0.22603-07 \\ c_1 &= 0.108713-02 & c_4 &= 0.171090-09 \\ c_2 &= -0.695706-05 & c_5 &= -0.144039-11 \end{aligned} \quad (13)$$

α is calculated from (13) by differentiating with respect to temperature. Representative families of such curves are shown in Figure 7. The value for α at 140 mW/cm^2 and 28°C for these cells is 0.11.

Uncertainties in the voltage output of the solar cell are due to uncertainties in intensity, cell temperature and instrumentation accuracy. Voltage uncertainties can be calculated using the empirical Patterson formulae. The open circuit voltage dependence of a solar cell is expressed as

$$V_{oc} = A(T) + B(T) \log H$$

where

$$A(T) = a_0 + a_1 T + a_2 T^2 + a_3 T^3 + a_4 T^4 + a_5 T^5$$

and

$$B(T) = b_0 + b_1 T + b_2 T^2 + b_3 T^3 + b_4 T^4 + b_5 T^5$$

$a_0 = 0.480654+03$	$b_0 = 0.801129+02$
$a_1 = -0.241702+01$	$b_1 = 0.118039+00$
$a_2 = 0.294965-02$	$b_2 = -0.224011-02$
$a_3 = -0.206159-04$	$b_3 = 0.140478-04$
$a_4 = -0.184560-06$	$b_4 = 0.816163-07$
$a_5 = 0.114636-08$	$b_5 = -0.548025-09$

(14)

The temperature coefficient of open circuit voltage is derived from (14) by differentiating: $\beta = (\partial V_{oc} / \partial T)_H$ and the intensity dependence of voltage is given by

$$\left(\frac{\partial V_{oc}}{\partial H} \right)_T = \frac{B(T)}{H \ln 10}$$

These coefficients apply to 2 ohm-cm cells, 2 x 2 cm x 0.46mm thick and strictly apply only to unirradiated cells.

The V_{oc} uncertainty is then

$$(dV_{oc})^2 = \left[\left(\frac{\partial V_{oc}}{\partial T} \right)_H dT \right]^2 + \left[\left(\frac{\partial V_{oc}}{\partial H} \right)_T dH \right]^2 + dM^2 \quad (15)$$

where V_{oc} is the open circuit voltage of the cell and dM is the uncertainty of the voltmeter calibration.

Families of curves showing $\partial V_{oc} / \partial T$ and $\partial V_{oc} / \partial H$ based on differentiating the Patterson formulae (14) are shown in Figures 8 and 9.

We use (15) to calculate an uncertainty dV_{oc} , then assume this voltage uncertainty applies over the entire I-V curve, but the percentage uncertainty varies over the curve as the inverse of the voltage. For $dT = \pm 1^\circ\text{C}$, $dH = 4.26 \text{ mW/cm}^2$ (3.04 percent of 140 mW/cm^2) and $dM = \pm 1 \text{ mV}$ (an uncertainty of ± 1 in the least significant digit of the digital voltmeter),

$$dV_{oc} = \left[(2.245 \times 1)^2 + (0.254 \times 4.26)^2 + (1)^2 \right]^{1/2} \text{ mV}$$

$$= 2.69 \text{ mV}$$

for a measurement at 28°C and intensity of 140 mW/cm^2 . Applying this voltage uncertainty to the 485 mV point, we compute a percentage uncertainty there of

$$\frac{dV}{V} = 0.55\%$$

The uncertainty in voltage quoted here is a function of several factors which nearly all arise because of an inability to repeat measurements and experimental conditions exactly from cell to cell. A 0.55 percent band exists on either side of the 485 mV setting. We should be willing to wager odds of 19 to 1 that any particular cell had its voltage output within that band when its current output reading was recorded. Since the band is finite, and since the slope of the I-V curve is approximately -0.25 mA/mV for 2 ohm-cm cells under these measurement conditions at the 485 mV point, this uncertainty in voltage will cause an additional uncertainty in the current reading of $-0.25 \times 2.69 = 0.67 \text{ mA}$ or approximately 0.56 percent. The nature of this uncertainty is to define an uncertainty area superimposed on any given point on the solar cell I-V curve. Such an area is illustrated in Figure 10 for a portion of a typical 2 ohm-cm Mariner '71 cell near the 485 mV point.

To properly calculate a 95 percent confidence limit we should add the current uncertainties due to the direct current uncertainty expressed in equation (12) and the indirect current uncertainty arising from the voltage uncertainty

$$\begin{aligned}\Delta I_T^2 &= \Delta I^2 + \left(\frac{dI}{dV} dV\right)^2 \\ &= \left(\frac{dI}{I} \times I_{sc}\right)^2 + (0.25 \times dV)^2 \\ &= (3.874)^2 + (0.673)^2\end{aligned}$$

$$\Delta I_T = 3.93 \text{ mA}$$

SECTION V

UNCERTAINTIES IN THE SOLAR PANEL CALIBRATION AT TABLE MOUNTAIN

When a panel has been assembled and has passed all its flight acceptance tests it is taken to Table Mountain, California, for the purpose of sunlight testing. It is instrumented to read panel temperature, pointed at the sun, and the entire I-V curve for the panel is recorded. A balloon flight standard cell (BFS) is used during the test to establish the incident solar intensity during the test. The panel I-V curve is used for categorizing the panels as to which will be flight panels (those best matched) and which will be flight spares. The panel I-V curve, which is the sum total output of an array of n cells in parallel by m cells in series, is compared with the I-V curve of a single solar cell of average output characteristics to calculate the manufacturing losses. Finally, the Table Mountain I-V curve is used to compute a standard I-V curve (presently at 145 mW/cm^2 and 60°C) of a single cell on the panel by dividing the panel currents by n and the panel voltages by m. This standard curve is then used in the solar panel prediction program from which the panel behavior is computed for all expected solar intensities and panel temperatures during its space mission. The accuracy of the prediction program will be discussed in a later section.

The uncertainties of the Table Mountain calibration arise from the original BFS calibration (± 1 percent), the temperature uncertainty of the BFS in use at Table Mountain ($\pm 2^\circ\text{C}$), the panel temperature uncertainty ($\pm 2.5^\circ\text{C}$) and the distribution of temperature across the panel (unknown). Uncertainties in the calibration of the current and voltage measuring equipment will also contribute. The uncertainty in the intensity measurement is calculated by using equation (7), equation (2) and inserting an additional term for instrumentation uncertainty. Assume the instrumentation uncertainty to be ± 1 digit in the least significant place or $\pm 1 \text{ mV}$ out of 60 mV (0.167 percent), and recall the $\pm 1^\circ\text{C}$ in the BFS temperature contributed 0.1 percent to compute:

$$\begin{aligned}\frac{dH}{H} &= \left[(0.01)^2 + (0.002)^2 + (0.00167)^2 \right]^{1/2} \times 100\% \\ &= 1.033\%\end{aligned}$$

In this case we can read the BFS cell with more assurance with the digital voltmeter because we do not have to contend with a dancing xenon arc as we do with the solar simulator.

The uncertainty in the panel current may be computed by modifying equation (6) to account for the n cells in parallel on the panel or panel section and adding a term for instrumentation accuracy, dM/M .

$$\left(\frac{dI_p}{I_p}\right)^2 = \left(\frac{dH}{H}\right)^2 + \left(\frac{n\alpha dT}{I_p}\right)^2 + \left(\frac{dM}{M}\right)^2 \quad (16)$$

The voltage uncertainty is computed by modifying equation (15) to account for the m cells in series on the panel or panel section and adding the term for instrumentation accuracy:

$$\left(\frac{dV_{oc}}{V_{oc}}\right)^2 = \left(\frac{m\beta}{V_{oc}} dT\right)^2 + \left[\frac{m}{V_{oc}} \left(\frac{\partial V_{oc}}{\partial H}\right)_T dH\right]^2 + \left(\frac{dM}{M}\right)^2 \quad (17)$$

If we assume an instrumentation uncertainty of 0.5 percent for both the voltage and current meters, and use appropriate test data taken from the July 17, 1970 Table Mountain testing of Mariner '71 panel S/N 019, Section E, ($n=10$, $m=78$, $I_{sc}=1.189$ amperes, $V_{oc}=41.66$ volts, $H=127.3$ mW/cm², $T_p=47.2^\circ\text{C}$), we compute

$$\frac{dI_p}{I_p} = \left[(0.01033)^2 + \left(\frac{10 \times 0.085 \times 2.5}{1.189 \times 10^3} \right)^2 + (0.005)^2 \right]^{1/2} \times 100$$

$$\frac{dI_p}{I_p} = 1.161\% \quad (18)$$

and

$$\frac{dV_{oc}}{V_{oc}} = \left[\left(\frac{78 (-2.28) 2.5}{41.66 \times 10^3} \right)^2 + \left(\frac{78 (0.277)}{41.66 \times 10^3} (0.01033 \times 127.3) \right)^2 + (0.005)^2 \right]^{1/2} \times 100 = 1.18\% \quad (19)$$

where we have used appropriate values for α , β , and $\partial V_{oc} / \partial H$ at 127.3 mW/cm^2 and 47°C of $0.085 \text{ mA}/^\circ\text{C}$, $-2.28 \text{ mV}/^\circ\text{C}$, and 0.277 mV/mW/cm^2 respectively, which again, were obtained from figures 7, 8, and 9 or from differentiating the Patterson expressions.

At the completion of the Table Mountain testing of a solar panel, the manufacturing losses are calculated. This is done by applying temperature and intensity corrections to correct the panel output to the temperature and intensity conditions at which the individual cells were measured. The panel I-V curve is transformed to a single cell curve by dividing the current by the number of cells in parallel and the voltage by the number of cells in series. The maximum power point of this transformed curve is compared with the maximum power point of the average single solar cell used in the panel. A percentage degradation is calculated and referred to as the manufacturing loss. Spacecraft power people quote from 3 to 10 percent manufacturing loss. JPL typically finds a 6 percent loss. Several comments are in order. The panel current output is measured more accurately at Table Mountain than is the output of the single cells because the light intensity is better known. This may be mitigated by a less accurate solar spectrum at Table Mountain due to absorption in the atmosphere of selective portions of the spectrum. The voltage output is less uncertain for the single cells because the temperature is known more precisely. A part of the loss may be simply due to the uncertainties in intensity, temperature, and instrumentation. It is assumed here that the same BFS is not used at Table Mountain as is used at the Cell Vendor's establishment to calibrate his SWS cells. Neither are the same voltmeters used for measuring voltage and current at the two sites. Some of the uncertainties would be reduced if the same voltmeters and BFS cells could be used at each site. This procedure would not eliminate the absolute uncertainties in either measurement,

but would eliminate constant offset type errors in making the comparison, and would make the comparison between the single cell measurements and panel measurements more meaningful.

SECTION VI

PREDICTING PANEL OUTPUT IN SPACE

A. CORRECTION FOR SOLAR INTENSITY AND PANEL TEMPERATURE

Predicting the panel output in space involves two types of corrections. The first is the correction for changing solar intensity and panel temperature. The second is for the effects of various environmental elements which damage the panel, namely electron and proton radiation damage and possibly UV degradation of the coverslide system. (Reference 7)

The prediction of solar panel output in space is made using the JPL computer program M132000. The calculational technique is based on the formulas of Sandstrom (References 8 and 9), on some unpublished work by Blake (Reference 10), and miscellaneous adjustments by several others. The various temperature and intensity coefficients in the program are derived from the parametric data of Yasui (Reference 11). A reference I-V curve is stored in the program which is applicable to the single solar cell/coverslide configuration of interest. Presently the I-V curve is for a Heliotek N/P 2 x 2 cm cell, 0.46 mm thick, 2 ohm-cm resistivity, with a 7940 fused silica coverslide 0.51 mm thick. The coverslide was mounted with RTV 602 adhesive. This is the configuration flown on Mariner '69 and '71. The reference I-V curve is for a solar intensity of 145 mW/cm^2 and a cell temperature of 60°C . It was derived from Mariner '71 panel measurements at Table Mountain (Reference 12) and therefore has all the inherent uncertainties of the Table Mountain measurements previously discussed as well as the uncertainties in correcting the experimental data to 145 mW/cm^2 and 60°C from the Table Mountain data (taken at approximately 125 mW/cm^2 and 50°C). Therefore all data on solar panel output from the program will have the uncertainties present that are discussed in this section, even any so-called uncorrected panel data at 145 mW/cm^2 and 60°C . The reference I-V curve consists of 30 I-V pairs spanning from well into the second current-voltage quadrant through the first quadrant and into the fourth quadrant.

The I-V curve for an arbitrary temperature intensity combination is found by translating the reference curve by the following equations:

$$I_1(J) = I(J) + I_{sc}(\text{ref}) \left(\frac{H_2}{H_1} - 1 \right) + n\alpha_2 (T_2 - T_1)$$

$$\Delta I = I_1(J) - I(J)$$

$$V_1(J) = V(J) - \beta_2 m (T_2 - T_1) - \Delta I (R_{s2} + 0.114) \frac{m}{n} - K_2 \frac{m}{n} (T_2 - T_1) I_1(J) \quad (20)$$

Here

$I(J)$ and $V(J)$ are current and voltage points on the reference I-V curve
 $I_1(J)$ and $V_1(J)$ are current and voltage points on the transformed I-V curve.

$I_{sc}(\text{ref})$ = reference curve short circuit current

H_2 = new solar intensity

T_2 = new cell temperature

H_1 = reference curve solar intensity

T_1 = reference curve cell temperature

α_2 = averaged short circuit temperature coefficient at T_2 and H_2 referenced to T_1

β_2 = averaged open circuit voltage temperature coefficient at T_2 and H_2 referenced to T_1

R_{s2} = solar cell series resistance at T_2

K_2 = solar cell curve shape correction factor at intensity H_2

m = number of cells in series on the panel

n = number of cells in parallel on the panel

These equations simply translate the whole I-V curve parallel to the current axis by the same amount that the short circuit current is translated with varying temperature and intensity. The I-V curve is translated parallel to the voltage axis by the same amount that the open circuit voltage is translated with temperature and intensity and by an additional amount equal to the IR drop across the panel calculated for the new current. If the equation for a single cell is desired, m and n are set equal to 1 and the factor of 0.114 is not added to R_{s2} . The 0.114 appears to be an adjustment found necessary to account for interconnect and panel harness resistance, and should probably be temperature-dependent.

Note that the "temperature coefficients" α and β are derived relative to 60°C only (reference 10), and must be changed if a reference curve at a different temperature is desired. These coefficients in their present form have been calculated in an approximate fashion and should be updated. The cell series resistance derivation was done by a standard technique originally suggested in reference 13. The technique must be carried out very carefully to avoid certain pitfalls and snares. The resistance is calculated using points from two I-V curves of the same solar cell illuminated at different intensities. The calculated resistance varies according to what illumination intensities happened to have been chosen by the experimenter. Typically the cell resistance measured in this manner will vary by about ± 0.05 ohm for the same cell, depending on the intensity levels used. The measurement should properly be done by examining a large number of cells and a least squares fit made to all the data in order to derive a temperature dependence and a 95 percent confidence envelope. The accuracy of the cell resistance values in use is not known nor are the confidence limits known.

After making temperature/intensity corrections using the α 's, β 's, and R_{s2} , it was found that the knee of the corrected I-V curve was improperly rounded. The curve shape correction coefficient, K_2 , was therefore included in formula (13) and was empirically adjusted to give the "best fit" (Reference 10)

to the laboratory parametric I-V curves. The criterion for establishing best fit is not stated. Neither are confidence limits established. The K_2 factors were found to be mainly a function of solar intensity.

The derived α 's, β 's, R_{s2} 's and K_2 's were used to recalculate (Reference 10) the original parametric data. Here transformations were made from a reference curve at 253 mW/cm² solar intensity and 60°C. A table of correlations was calculated. The correlation table appears approximately correct. Maximum deviations of the calculated I_{sc} , V_{oc} , and P_{max} from the laboratory values were 1.36 percent, 1.36 percent, and 1.63 percent respectively, but these values may be optimistic. The optimism may be expressed by using the maximum deviations as 95 percent confidence limits. The original parametric data of Yasui were obtained with a sample size of 13 solar cells. He computed statistical parameters for the cells including 95 percent confidence limits. Considering only the temperature-solar intensity regime bounded by -20°C, 60°C, 50 mW/cm² and 250 mW/cm² which is of primary interest here, maximum 95 percent confidence limits of 0.97 percent and 0.33 percent were found for I_{sc} and V_{oc} respectively. Prediction errors found by Blake over this same temperature-solar intensity regime are 1.13 percent for I_{sc} and 0.78 percent for V_{oc} . The uncertainty of the predicted solar panel current may be expressed as

$$\frac{dI_p}{I_p} = \frac{dH}{H} + \frac{\alpha_o dT_t}{I_t} + \frac{n\alpha dT_p}{I_p} + \left(\frac{dI}{I}\right)_{TM} + S_I + e_I \quad (21)$$

where S_I is the statistical 95 percent confidence limit of the parametric current data and e_I is the prediction error in current due to the approximate nature of the computing technique. dT_t is the temperature uncertainty of the cells in the test chamber during the parametric study ($\pm 1^\circ\text{C}$) with a corresponding α_o and current I_t , dT_p is the solar panel temperature uncertainty with an α appropriate to (H, T_p) . n is the number of cells connected in parallel on the panel or panel section. $(dI/I)_{TM}$ is the uncertainty in measuring the solar panel current at Table Mountain. This term must be added in if the reference I-V curve in the computer program is derived from the Table Mountain data as is the present practice.

The solar intensity uncertainty in equation (21) consists of two parts. One is the uncertainty of the simulator intensity when generating the parametric data and is calculated by using appropriate values in equations (8) and (9), namely 1.0 percent for the BFS calibration uncertainty, 1.0 percent for the uncertainty due to simulator drift, 0.1 percent for the uncertainty due to BFS temperature control and measurement, and 0.5 percent for the uncertainty associated with the calibration and reading of the digital voltmeter. The total intensity uncertainty of the simulator when generating parametric data therefore is:

$$\left(\frac{dH}{H}\right)_{\text{par}} = \left[(0.01)^2 + (0.01)^2 + (0.001)^2 + (0.005)^2 \right]^{1/2} \times 100 = 1.50\%$$

The other part comes from the uncertainty in solar intensity due to uncertainties of spacecraft position with respect to the sun and the incidence angle of sunlight on the panels. Uncertainties in the solar constant do not come into play here because all measurements are ratioed to balloon flight standard cells which were measured at air mass zero at one solar constant, whatever its value. The solar intensity incident on the panel is calculated by

$$H = \frac{K \cos \theta}{r^2} \quad (22)$$

where r is the spacecraft to sun distance, θ is the incidence angle, and K is a constant.

$$\left(\frac{dH}{H}\right)_{s/c} = \frac{-2}{r} dr - \tan \theta d\theta \quad (23)$$

On Mariner '71 $d\theta$ was about 1/4 degree (4.36×10^{-3} radian) and dr was approximately 10 km. r is of the order of 10^8 km. Therefore

$$\left(\frac{dH}{H}\right)_{s/c} = \left[\left(\frac{2 \times 10}{10^8}\right)^2 + (4.36 \times 10^{-3} \times 4.36 \times 10^{-3})^2 \right]^{1/2} \times 100 = 0.0019\%$$

and the combined intensity uncertainties in solar intensity are

$$\frac{dH}{H} = \left[\left(\frac{dH}{H}\right)_{\text{par}}^2 + \left(\frac{dH}{H}\right)_{s/c}^2 \right]^{1/2} = 1.50\% \quad (24)$$

It is apparent that the uncertainty in the solar intensity incident on the spacecraft solar panels is negligible in comparison to the other uncertainties.

As an example of the application of equation (21), assume we want to find the uncertainty in the predicted solar panel current at 100 mW/cm^2 solar intensity and panel temperature of 0°C . The appropriate α and I_{sc} for these conditions are $0.11 \text{ mA}/^\circ\text{C}$ and 90 mA (for a single 2 ohm-cm solar cell). Assume a solar panel temperature uncertainty of 5°C and use the value computed in equation (18) for the relative current uncertainty in the Table Mountain measurements (0.01161) and calculate a total uncertainty in the predicted current as follows:

$$\begin{aligned} \frac{dI_p}{I_p} = & \left[(0.015)^2 + \left(\frac{0.11 \times 1}{90}\right)^2 + \left(\frac{0.11 \times 5}{90}\right)^2 + (0.01161)^2 + (0.0097)^2 \right. \\ & \left. + (0.0113)^2 \right]^{1/2} \times 100 = 2.49\% \end{aligned} \quad (25)$$

In a similar fashion, the uncertainty in voltage is derived from a modification of equation (15) to give

$$\frac{dV_{oc}}{V_{oc}} = \left(\frac{1}{V_{oc}} \frac{\partial V_{oc}}{\partial T} dT_t \right) + \left(\frac{1}{V_{ocp}} \frac{\partial V_{oc}}{\partial T} dT_p \right) + \left(\frac{1}{V_{ocp}} \frac{\partial V_{oc}}{\partial H} dH \right) + \left(\frac{dV_{ocp}}{V_{ocp}} \right)_{TM} + S_V + e_V \quad (26)$$

S_V is the 95 percent confidence limit for the parametric voltage data, e_V is the computer voltage prediction error, V_{ocp} is the panel open circuit voltage, and

$$\left(\frac{dV_{ocp}}{V_{ocp}} \right)_{TM}$$

is the uncertainty in measuring the solar panel voltage at Table Mountain. This term must be added in if the reference I-V curve in the computer program is derived from the Table Mountain data as it is in present practice. dH is the value calculated using equation (24).

As an example of the application of equation (26), we will calculate the uncertainty in the predicted solar panel voltage at 100 mW/cm^2 solar intensity and panel temperature of 0°C . Appropriate values for the required parameters are: $V_{oc} = 641 \text{ mV}$, $dH = 0.015 \times 100 \text{ mW/cm}^2 = 1.5 \text{ mW/cm}^2$, $(\partial V_{oc}/\partial T) = -2.18 \text{ mV}/^\circ\text{C}$, $dT_t = 1^\circ\text{C}$, $dT_p = 5^\circ\text{C}$, $(\partial V_{oc}/\partial H) = 0.35 \text{ mV-cm}^2/\text{mW}$, $s_V = 0.0033$, $e_V = 0.78$ percent (Blake's "maximum" prediction error of V_{oc}), and $(dV_{ocp}/V_{ocp})_{TM} = 0.0118$ from equation (19).

$$\frac{dV_{oc}}{V_{oc}} = \left[\left(\frac{-2.18 \times 1}{641} \right)^2 + \left(\frac{-2.18 \times 5}{641} \right)^2 + \left(\frac{0.35 \times 1.5}{641} \right)^2 + (0.0118)^2 + (0.0033)^2 + (0.0078)^2 \right]^{1/2} \times 100 = 2.26\% \quad (27)$$

Since the entire I-V curve is translated along both axes by the computer program and the amount of the translation has been computed using I_{sc} and V_{oc} behavior as the basis, errors in I_{sc} and V_{oc} apply to each point on the curve. An error of 1 mA in I_{sc} , for example, is an error of 1 mA all along the I-V curve, and it is a higher percentage at all other points. Similarly for V_{oc} . An uncertainty in power is computed simply as

$$\left(\frac{dP_m}{P_m}\right)^2 = \left(\frac{dV_{oc}}{V_{oc}} \frac{V_{oc}}{V_{mp}}\right)^2 + \left(\frac{dI_{sc}}{I_{sc}} \frac{I_{sc}}{I_{mp}}\right)^2 \quad (28)$$

at the maximum power point. Note that this is in effect an approximation of the four sided area of Figure 10 by a rectangle.

The hypothetical Mariner '71 panel section for which we have evaluated formulas (21) and (26) at 100 mW/cm^2 and 0°C (an $m \times n$ array of 78×10 cells) would have a maximum power of 35.5 watts at 42.26 volts and 0.839 amperes under these conditions computed by using the parametric data of reference 11 but ignoring manufacturing losses. Correspondingly, approximate I_{sc} and V_{oc} values would be 0.92 amps and 50.0 volts. $dI_{sc} = 0.92 \times 0.0249 = 0.0229$ amps and $dV_{oc} = 50.0 \times 0.0226 = 1.13$ volts. Applying equation (28), the uncertainty in maximum power due to the prediction process is

$$\frac{dP_m}{P_m} = \left[\left(\frac{1.13}{42.26}\right)^2 + \left(\frac{0.0229}{0.839}\right)^2 \right]^{1/2} \times 100 = 3.82\% \quad (29)$$

This is a typical power prediction uncertainty for Mariner type solar panels operating between Venus and Mars when the panel components have been measured using today's techniques. A summary of the contributions to the error expressed in equation (28) is shown in Table I.

Squaring and adding the values in the columns to the right will give relative uncertainties in I_{sc} and V_{oc} respectively. The examples are for a calculation of panel performance at 100 mW/cm^2 and 0°C . Other numbers

Table I. Sources of Solar Panel Uncertainty

Parameter		Uncertainty	
I.	I_{sc} SHORT CIRCUIT CURRENT		
	dH (Simulator)	0.015	
	BFS calibration	0.01	
	BFS temperature	0.001	
	DVM calibration and read	0.005	
	Simulator drift	0.01	
	dH (Solar Intensity)	1.9 - 05	
	S/C - Sun distance	2.0 - 07	
	Pointing error	1.9 - 05	
	dH (Total)		0.015
	dT_t (Parametric Data)*	1.0°C	
	$\left(\frac{\partial dT_t}{I}\right)$ at (100, 0)		1.22-03
	dT_p (S/C panel temperature)*	5.0°C	
	$\left(\frac{\partial dT_p}{I}\right)$ at (100, 0)		6.11-03
	dI/I (Table Mountain Reference Curve)		0.01161
	s_I (Parametric statistics)		0.0097
	e_I (M132000 approximation)		0.0136
II.	V_{oc} OPEN CIRCUIT VOLTAGE		
	dH (Simulator + Solar Intensity)		
	$\left(\frac{\partial V_{oc}}{\partial H}\right)_T \frac{dH}{V_{oc}}$ at (100, 0)	0.015	8.19-04
	dT_t (Parametric Data)*	1°C	
	$\left(\frac{\partial V_{oc}}{\partial T}\right)_H \frac{dT_t}{V_{oc}}$ at (100, 0)		3.40-03
	dT_p (S/C panel temperature)*	5°C	
	$\left(\frac{\partial V_{oc}}{\partial T}\right)_H \frac{dT_p}{V_{oc}}$ at (100, 0)		0.017
	$\frac{dV_{oc}}{V_{oc}}$ (Table Mountain Reference)		0.0118
	s_V (Parametric statistics)		3.30-03
	e_V (M132000 approximation)		1.36-02
*Starred data is absolute, other non-starred data is relative (xxx, yy) means at solar intensity of xxx mW/cm ² , and yy°C. The quantities in the right column are based on or derived from the quantities in the middle column.			

must be substituted for the five values in the table written with (100, 0). The values for e_I and e_V in the table are pertinent to the temperature-solar intensity regime -40 to 140°C , and 25 mW/cm^2 to 540 mW/cm^2 . Lesser values than these were used in the example calculated because we were there restricting ourselves to a smaller temperature-solar intensity regime, and the maximum value for the restricted regime was used. After finding the relative uncertainties in panel voltage and current, equation (28) is used to find the uncertainty in maximum power.

B. CALCULATION OF A MISSION POWER PROFILE

This section will treat the calculation of solar panel output during the course of a mission, allowing for various environmental degradation factors and the changing temperature and solar intensity. An initial I-V curve for the panel just after launch is assumed. If the panel is to be manufactured from the same kind of solar cells as was a previously built well known panel, the starting I-V curve may be taken from that panel. This initial curve may be obtained from the I-V curve of a single solar cell with the voltage multiplied by m , the current multiplied by n and the resultant curve modified by some sort of panel assembly loss factor. After a panel has been built and tested at Table Mountain a better estimate of an initial I-V curve may be obtained by correcting to initial space conditions using the techniques of M132000. This initial I-V curve thereafter is translated parallel to the voltage and current axes by the program to take into account the known cell response to the changing environments. This procedure has the inherent assumption that the environments produce little change in the temperature and intensity coefficients of voltage and current. It also assumes there is no significant fluence of low energy protons incident on unprotected cell surface areas. (Significant fluences would be, for example, 10^{11} p/cm^2 of 0.2 MeV protons incident a 10 mil gap near the bus bar.)

The first step in calculating the panel output is to calculate the response curve as a function of mission time assuming no environmental degradation. This assumes that the time variation of the panel temperature and the incident solar intensity is known. The uncertainties in I_{sc} , V_{oc} , and P_{max} may be assigned to the calculated time dependent curves at whatever confidence level

desired by using the principles discussed in this paper. The result of the M132000 calculation may be considered to be the predicted average I-V curve as a function of time and the uncertainty calculation will establish a band of curves above and below the average curve, each band corresponding to a particular confidence limit.

The non-degraded profile curve will in general require modification to account for degrading environments. A degrading environment is considered to be one which produces an irreversible and usually deleterious effect. The basic technique is to consider each environment individually and calculate its modification to the current and voltage of the panel. For example, suppose the panel must fly through two environments, A and B, during the mission. Also suppose environment A alone would reduce the solar cell short circuit current by X_A percent, and the open circuit voltage by Y_A percent, and environment B alone would reduce the short circuit current by X_B percent and the open circuit voltage by Y_B percent. Then the resulting I-V curve can be found by translating the undegraded I-V curve. Translate the current by an amount

$$I_{sc} \left(1 - \frac{X_A}{100}\right) \left(1 - \frac{X_B}{100}\right) \quad (30)$$

and the voltage by an amount

$$V_{oc} \left(1 - \frac{Y_A}{100}\right) \left(1 - \frac{Y_B}{100}\right) \quad (31)$$

to get the new I-V curve. I_{sc} and V_{oc} are the undegraded short circuit current and open circuit voltage of the panel assumed to be corrected for intensity and temperature. The maximum power will be determined from the resultant curve. If more than two degrading environments are involved, additional multiplicative terms are appended to equations (30) and (31).

The degrading environments likely to require attention are radiation and the mysterious monotonic degradation (hereinafter referred to as MM) which is seen on some spacecraft and is apparently independent of bulk damaging radiation (Refs. 7 and 16). Other environments that may need attention on some

missions are micrometeoroids, thermal cycling, and ultraviolet interaction with coverslide adhesives or optical coatings.

For satellites orbiting the Earth in the Van Allen belts, the radiation fluence increases more or less monotonically as the spacecraft stays in Earth orbit with an occasional fluence of solar flare protons added from time to time. The interplanetary missions flown by JPL so far have not been subjected to radiation fluences of consequence. These spacecraft receive only minimal radiation doses as they pass through the Van Allen belts. Their major radiation exposure results from the sporadic emanations from the Sun when it emits protons during a solar flare. Therefore the JPL panel designer does not usually have a smooth curve detailing radiation exposure as a function of time. Instead, he will most likely have a curve which plots proton fluence as a function of the probability of receiving less than that fluence. A fluence-energy spectrum definition will also be given in some form. It is usually up to the individual panel designer to select the radiation risk he wishes to include in his design, by selecting a probability level on the fluence curves. He must also assume that the total radiation dose will occur all at once, since nearly the entire exposure may be due to the protons emitted during a single solar event. He must further assume that this event will occur at the least optimum time, probably when the spacecraft is closest to the sun since the fluence goes roughly as $1/r^2$, or perhaps just prior to or during the peak power demand of the spacecraft.

To properly factor the radiation damage into the panel power prediction, the radiation environment for 50 percent probability of occurrence should be selected. This amount of radiation should be coupled with the standard techniques for computing solar cell degradation (References 14 and 15) and a percentage remaining P_{\max} computed using equations (30) and (31). This fraction should then be multiplied by the predicted time dependent performance curve for a non-irradiated panel. The 95 percent confidence limit of panel degradation due to radiation may be established as follows: Take the radiation level on the fluence vs probability curve at the point where the probability is 95 percent that the spacecraft will receive no more than this level. Calculate the cell degradation and the percentage electrical power remaining as before.

Multiply this fraction by the predicted time dependent performance curve for a non-irradiated panel. The difference in power defined by subtracting the powers calculated using the two fluences gives a dP_r which may be expressed as a relative power, squared, added to the square of the power uncertainty calculated in equation (28), and square rooted to give an overall uncertainty. Similar procedures may be used for I_{sc} and V_{oc} and for other confidence limits.

This procedure should be followed for factoring in the panel degradation for other environmental agents. Establish an average degradation due to the effect of the environment, then find some way of calculating a degradation band encompassing the desired confidence level. If the band width is expressed in maximum power, then the uncertainty may be added to the previously computed maximum power uncertainty by computing the relative uncertainty (using half the band width), squaring, and adding to the square of the uncertainty due to other effects and taking the square root of the total to give the total uncertainty.

If the designer has used an accurate starting I-V curve and followed the above steps he has now effectively arrived at a family of curves which give solar panel output as a function of mission time. Each curve of the family corresponds to a different level of confidence that the panel will meet or exceed the plotted power level. The whole family of curves may be moved up or down (translated parallel to the power axis), by simply adding or subtracting the total number of cells on the panel to make slight adjustments in the power profile. Large translations will not be accurate because of the differing ways in which m and n affect the power uncertainty of equation (28). The family of curves may be superimposed on the required power profile curve for the mission and translated up or down until the panel power output curve exceeds the power requirement curve at all times in the mission. Comparison will be made at the confidence level dictated by the project philosophy. If a substantial translation of the original calculated curve has been necessary to give the proper sizing, a recalculation of the family of curves will be necessary with the new values of n and m . Of course, if there is only one point in the mission where the power demand and power available curves may cross, then the entire set of calculations required to size the panel may be performed at that point. Having established n and m , the calculation of the family of power profile curves may be completed.

The mysterious monotonic radiation has been observed on the IDCSC spacecraft flying at synchronous altitude (Reference 7) and on Mariners 6, 7, and 9 (Reference 16). Patterson reports in reference 16 that the MM degradation on these Mariners has been fairly repeatable. The MM degradation has been referred to as uV degradation, mainly because better explanations have not been forthcoming. Other possibilities exist. All the IDCSC spacecraft used a primer and the Dow XR-6-3489 adhesive in mounting the coverslides. RTV-602 adhesive was used to mount the Mariner coverslides, but no primer was used. The IDCSC spacecraft used 10 ohm-cm Heliotek cells, the Mariners used 2 ohm-cm Heliotek cells. There is enough difference in the two solar cell systems so that the MM degradation seen on the two spacecraft could arise from different causes, or a combination of the same causes but a different mix. For example the IDCSC cells may be degrading because of a true uV degradation in the coverslide primer. Both spacecraft may suffer additional degradation due to uV degradation of the adhesive or optical coatings. Both may very likely be degrading because of contamination on the surfaces of the coverslides which darkens in the presence of radiation. Contaminants may arise from the spacecraft itself or from the vacuum chambers where the spacecraft were environmentally tested. An Air Force Tactical Communications Satellite (TACSAT) built by Hughes Aircraft Company did not experience the MM degradation. On this spacecraft, all the spaces between solar cells are fully grouted with an epoxy, and this panel was thoroughly cleaned with a mild abrasive after environmental testing and prior to launch. Surface contamination from the environmental vacuum chamber was probably removed quite effectively, but the cleaning was severe enough so that the uV cutoff filters on the coverslide could have been injured or removed. (Reference 17)

At any rate the MM degradation which has been repeatable, may not be repeatable or predictable in the future if panel assembly and environmental testing procedures are changed. The cause of this degradation should be investigated.

SECTION VII
RECOMMENDATIONS

1. Coverglasses should be applied to solar cells prior to the series of solar cell measurements to be used for matching the cells into submodules.
2. An investigation should be launched to determine the reason why there is so much scatter in the solar cell short circuit current loss due to glassing, and to try to find methods of reducing the scatter. One possible method is the use of TiO_x antireflection coatings on the solar cells instead of SiO .
3. Rewrite the JPL Solar Panel Prediction program (M132000). The revised program should be tied more directly to the original parametric data generated in the simulation laboratory. For example it would be better to have a table of parametric data for I_{sc} as a function of intensity and temperature from which I_{sc} at all intermediate intensities and temperatures could be interpolated. As it is now, several factors must be calculated from the parametric data and then put into M132000 before the program can be used. The program should have the capability of calling a radiation degradation subroutine to calculate the effect of any radiation environment on the electrical parameters of the panel. Other subroutines may be added, for example, a routine to compute coverslide darkening as a function of uV exposure if it can be proven that a functional relationship exists.
4. Tighten up the specification on setting up the simulator intensity at the solar cell vendor's establishment. The procedures currently in use give an enormous uncertainty in the simulator intensity.
5. Investigate carefully the exact cause of the mysterious monotonic degradation of the solar panels and the $I_{sc} - I_{scr}$ transducers on the Mariner solar panels.

REFERENCES

1. S. J. Kline and F. A. McClintock, Mechanical Engineering, Vol. 75, (Jan. 1953), p. 3.
2. W. J. Dixon and F. J. Massey, Jr., "Introduction to Statistical Analysis," McGraw-Hill, New York, 1957.
3. E. L. Crow, F. A. Davis, and M. W. Maxfield, "Statistics Manual," Dover Publications, New York, 1960.
4. JPL Specification SS500608, Rev. B, "Spacecraft Components, Definitions of Requirements for Photometalic Silicon Solar Cells (Types A, B, C, and D) Detail Specifications For," Jet Propulsion Laboratory, Pasadena, Calif., December 12, 1967.
5. R. Mueller, "Effect of X-25 Solar Simulator Color Ratio Upon Solar Cell Electrical Output," JPL Interoffice Memorandum No. 342-68-B-221, Jet Propulsion Laboratory, Pasadena, Calif., August 21, 1968.
6. R. E. Patterson, R. K. Yasui, and B. E. Anspaugh, "The determination and Treatment of Temperature Coefficients of Silicon Solar Cells for Interplanetary Spacecraft Application," Proceedings Seventh IECEC Conference, San Diego, Calif., Sept. 25-29, 1972.
7. W. T. Picciano, and R. A. Reitman, "Flight Data Analysis of Power Subsystem Degradation at Near Synchronous Altitude," Philco-Ford Report No. WDL-TR4223, Palo Alto, Calif., July, 1970.
8. J. D. Sandstrom, "A Method for Predicting Solar Cell Current-Voltage Characteristics as a Function of Incident Solar Intensity and Cell Temperature," Technical Report TR 32-1142, Jet Propulsion Laboratory, Pasadena, Calif., July 15, 1967.
9. J. D. Sandstrom, "Electrical Characteristics of Silicon Solar Cells as a Function of Cell Temperature and Solar Intensity," Conference Paper Presented at IECEC Meeting, Boulder Colorado, Aug. 1968.
10. F. A. Blake, "Solar Cell Performance; $5-540 \text{ mW/cm}^2$, $\pm 140^\circ\text{C}$." Unpublished Technical Report, Jet Propulsion Laboratory, Pasadena, Calif., Feb. 26, 1970.
11. R. G. Ross, Jr., R. K. Yasui, W. Jaworski, L. C. Wen, and E. L. Cleland, "Measured Performance of Silicon Solar Cell Assemblies Designed for Use at High Solar Intensities," Technical Memorandum 33-473, Jet Propulsion Laboratory, Pasadena, Calif., March 15, 1971.
12. W. Hasbach, "Private Communication."
13. M. Wolf and H. Rauschenbach, "Series Resistance Effects on Solar Cell Measurements," Advanced Energy Commission, Vol. 3, 1963, Great Britain.

14. W. C. Cooley and M. J. Barrett, "Handbook of Space Radiation Effects on Solar Cell Power Systems," NASA Contract NASW-1427, 1968.
15. J. R. Carter and H. Y. Tada, "Solar Cell Radiation Handbook," TRW Report 21945-6001-RU-00, JPL Contract No. 953362, June 28, 1973 (a JPL internal document).
16. R. E. Patterson, "Design and Flight Performance Evaluation of the Mariners 6, 7, and 9 Short-Circuit Current, Open-Circuit Voltage Transducers, JPL Technical Report," To Be Published.
17. E. Stoeffel, Hughes Aircraft Co. "Private Communication."

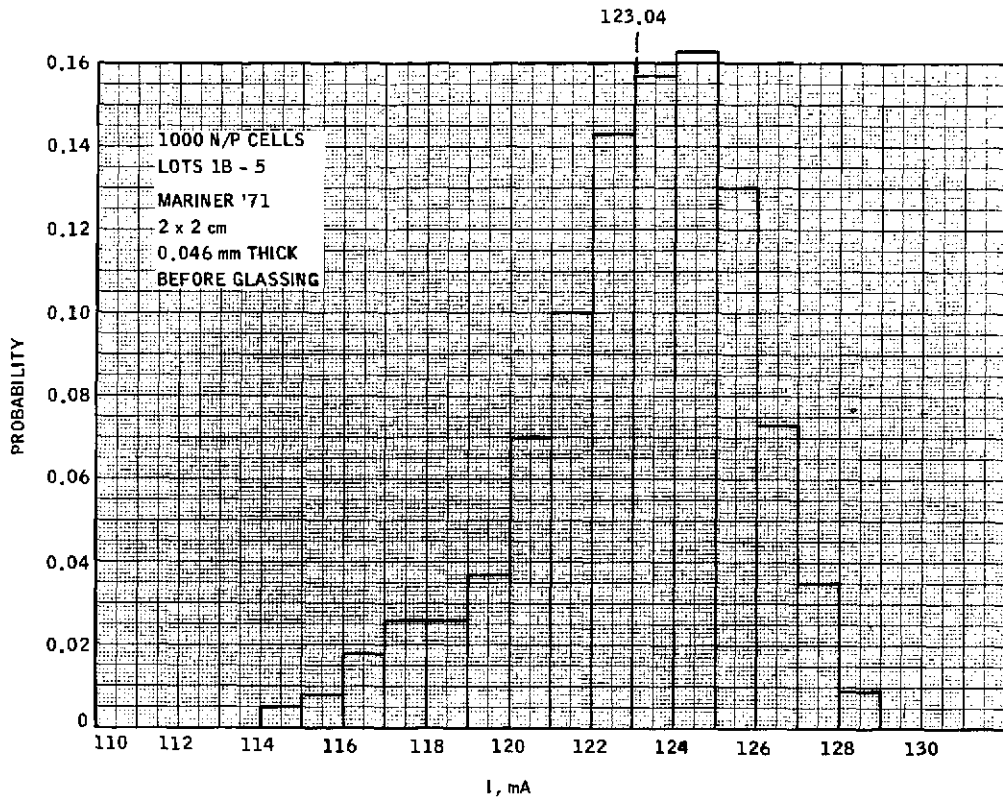


Fig. 1. Current at 0.485 volts, distribution for 2-ohm-cm cells

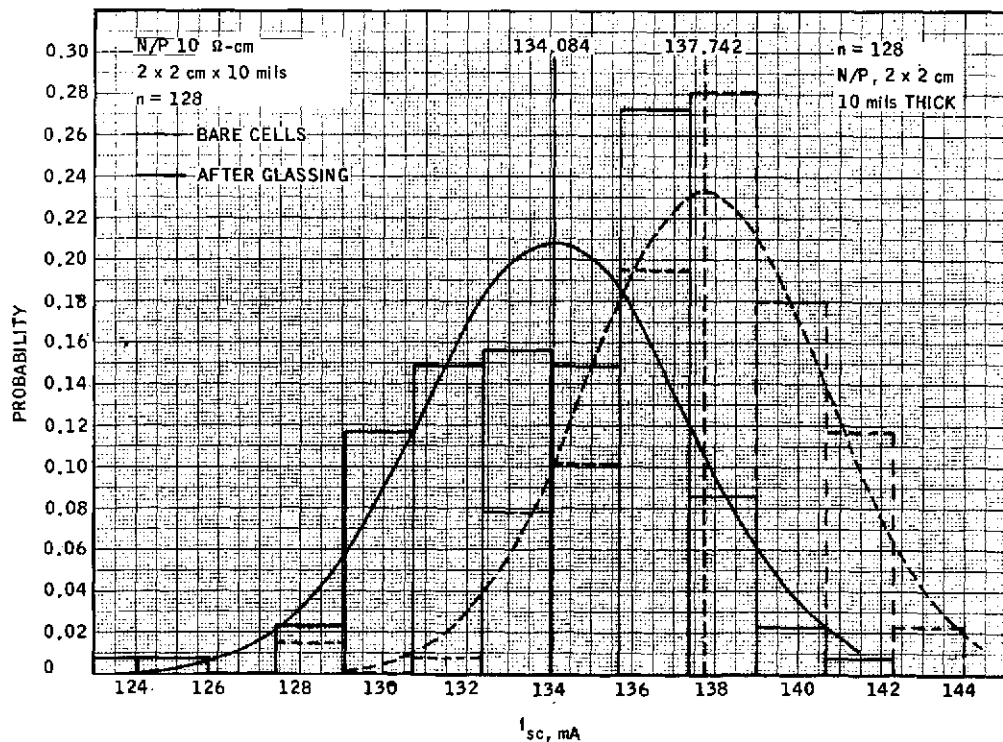


Fig. 2. Short circuit current distribution of 10-ohm-cm solar cells before and after glassing with 6-mil microsheet

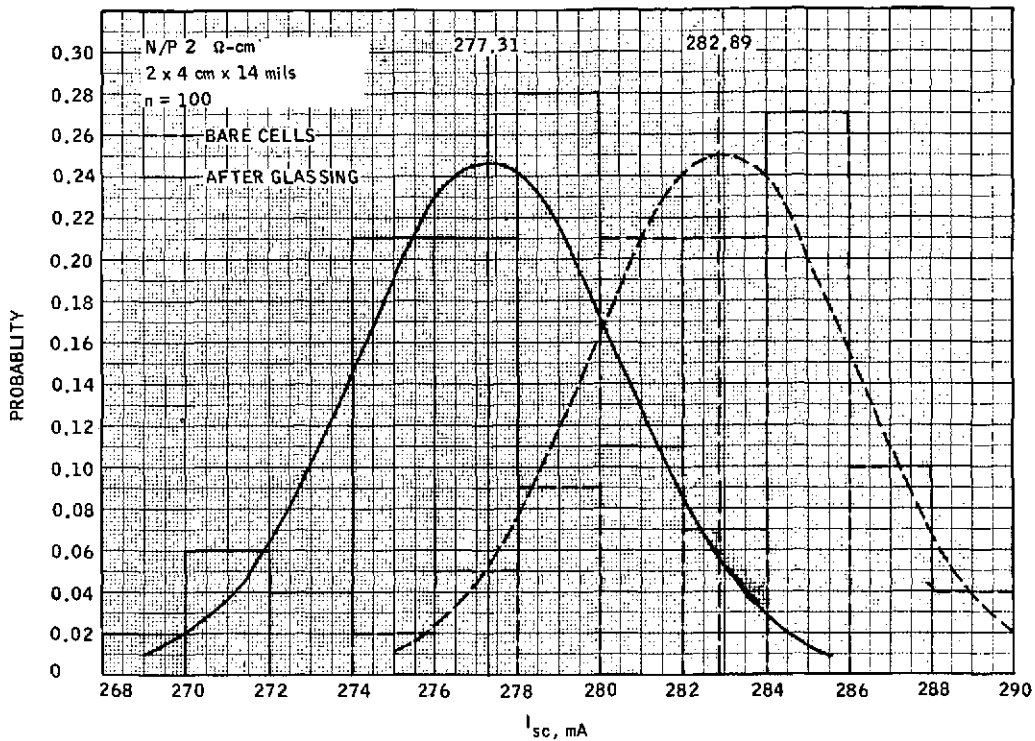


Fig. 3. Short circuit current distribution of 2-ohm-cm solar cells before and after glassing with 6-mil 7940 fused silica

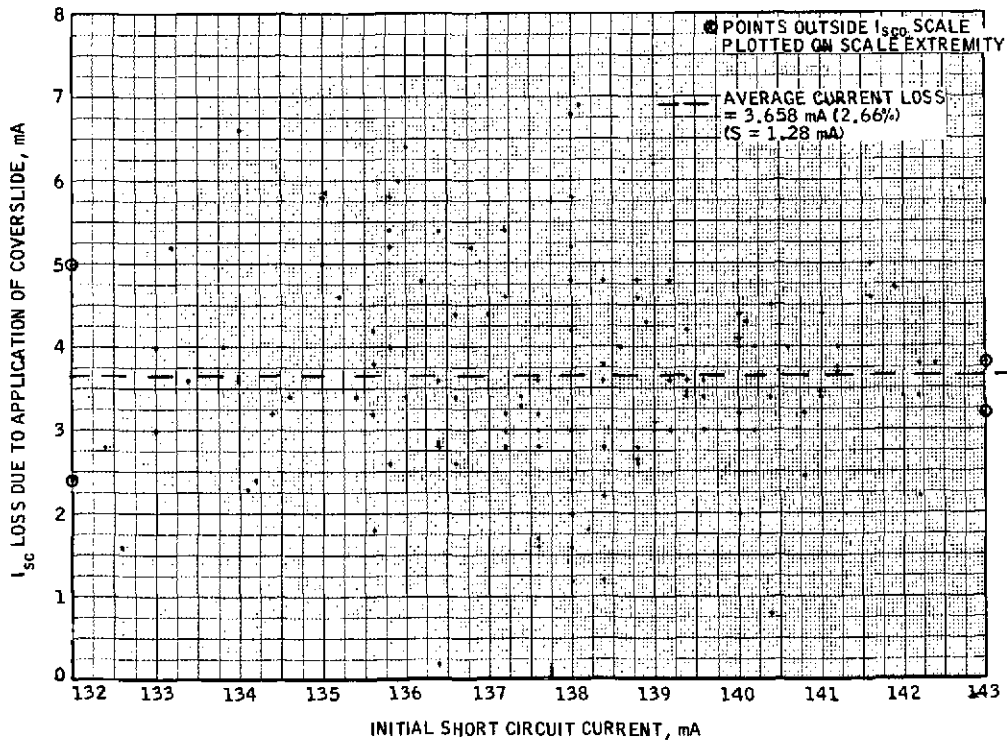


Fig. 4. Current reduction after coverslide mounting (2 x 2 cm cells)

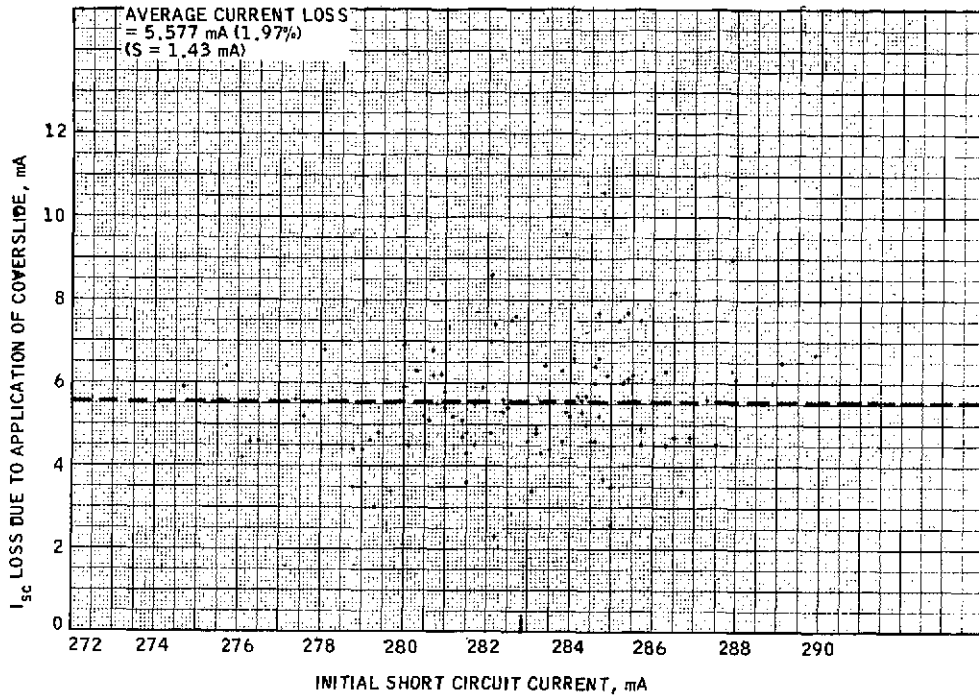


Fig. 5. Current reduction after coverslide mounting (2 x 4 cm cells)

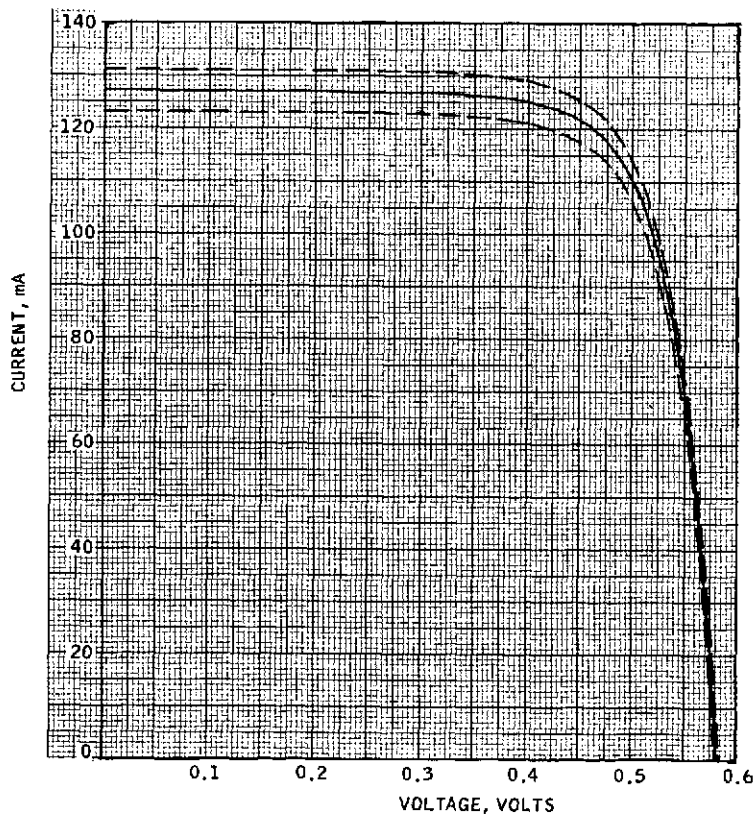


Fig. 6. 95% current confidence band on a 2-ohm-cm solar cell

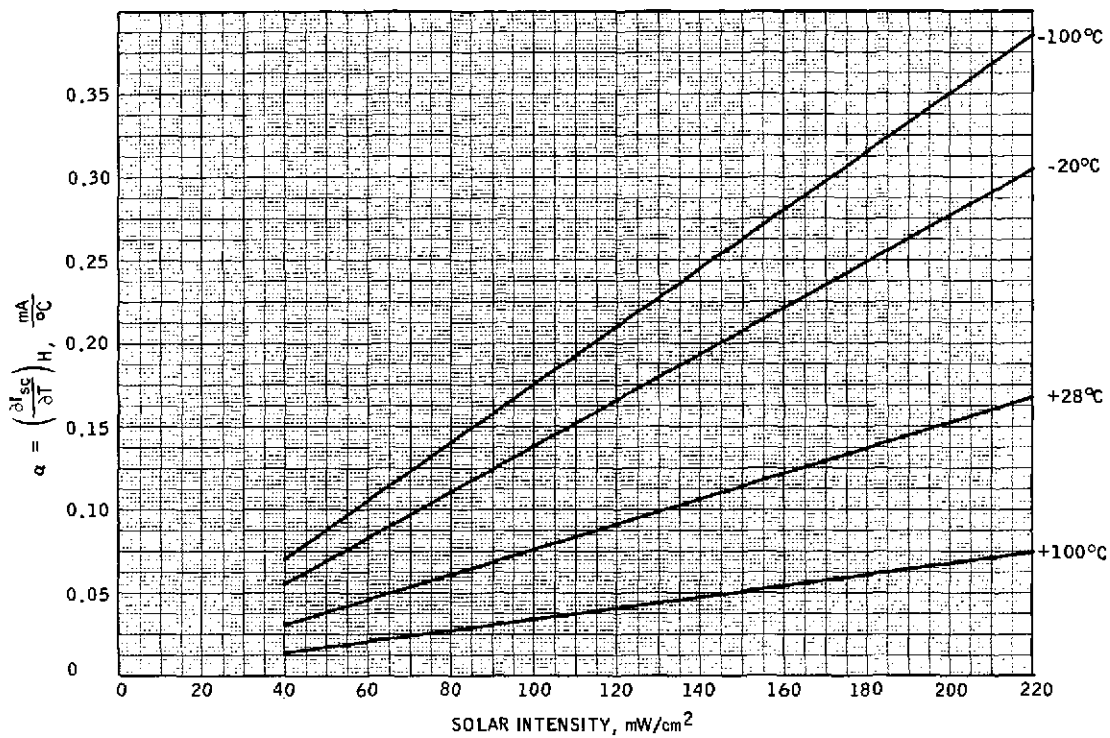


Fig. 7. $\alpha = (\partial I_{sc}/\partial T)_H$ based on differentiating Patterson's expression

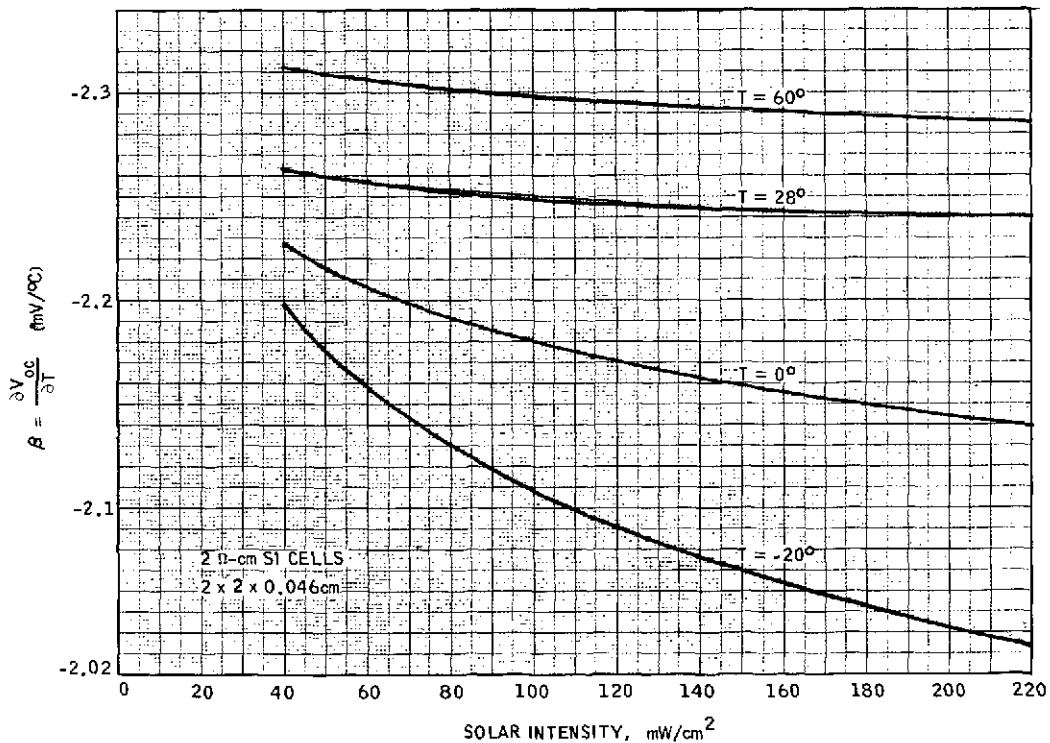


Fig. 8. $(\partial V_{oc}/\partial T)_H$ based on differentiating Patterson's expression

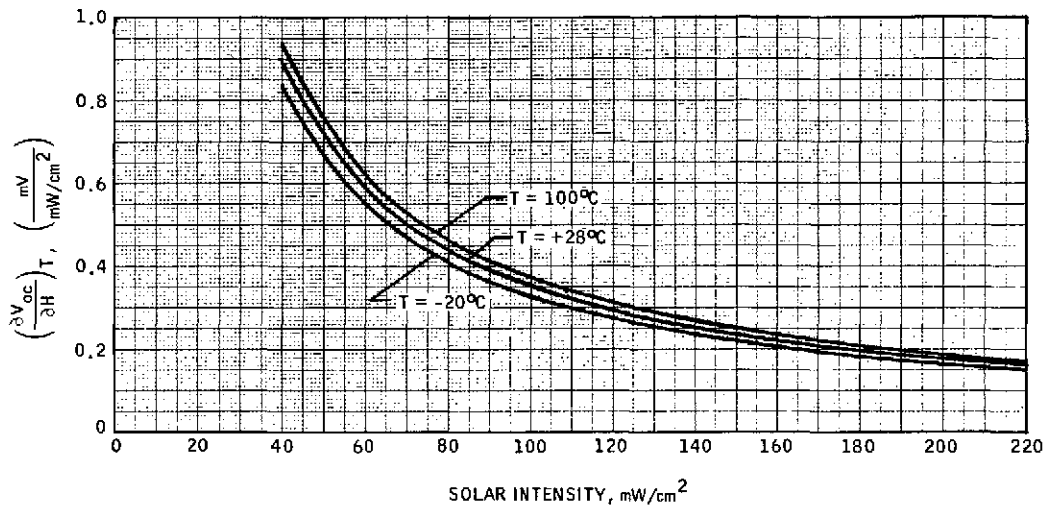


Fig. 9. $(\partial V_{oc}/\partial H)_T$ based on differentiating Patterson's expression

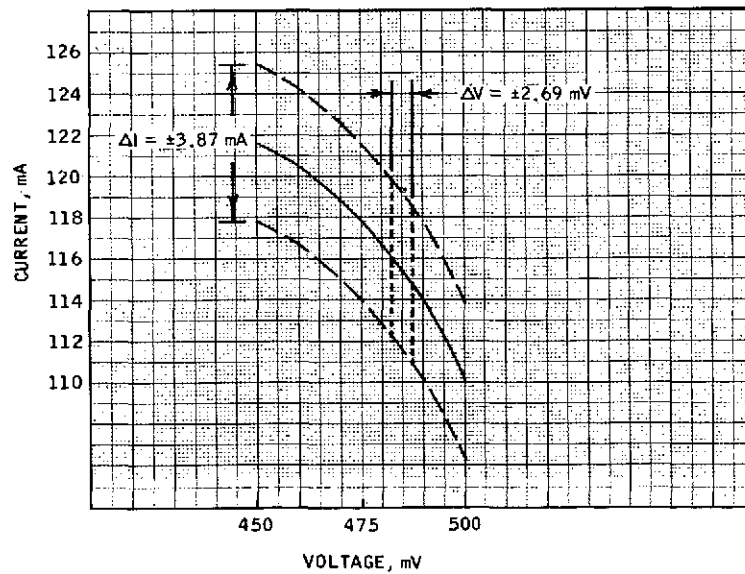


Fig. 10. Portion of 2-ohm-cm solar cell I-V curve near P_{max} for AMO, $28^\circ C$